Modified small-world networks as models of liquid and amorphous selenium

Thorsten Koslowski,[1,*] Michaela Koblischke,[1] and Alexander Blumen[2]
[1]*Institut für Physikalische Chemie, Universität Freiburg, Albertstraße 23a, D-79104 Freiburg, Germany*
[2]*Theoretische Polymerphysik, Universität Freiburg, D-79104 Freiburg, Germany*
(Received 1 October 2001; revised manuscript received 19 March 2002; published 14 August 2002)

In this work, we present a model of the disordered phases of selenium based upon ideas akin to small-world networks. This model accounts for the description of defect centers of liquid and amorphous Se, which can be introduced in a controllable manner in a broad interval of concentrations. The electronic structure is described by a tight-binding Hamiltonian, which is extended by a Hubbard term to take the influence of an effective electron-electron interaction into account. The resulting electronic structure problem is solved self-consistently. The electronic structure is analyzed in terms of the density of states, the charge order originating from defect states, the charge distribution function, and the localization properties of the eigenfunctions. Only bipolaron states—which compensate the charge of anionic dangling bonds—and positively charged centers with a threefold coordination give rise to impurity states within the band gap of the unperturbed system: The latter species corresponds to one of the defects of the Kastner, Adler, and Fritzsche model of selenium. Within the models studied here, states corresponding to negatively charged singly coordinated atoms lie deep within the bulk of the density of states, and their positively charged counterparts are not observed at all.

DOI: 10.1103/PhysRevB.66.064205 PACS number(s): 71.23.−k, 71.55.Cn, 72.15.Rn, 72.80.Ph

I. INTRODUCTION

The issue of the microscopic and electronic structure of Se in its disordered phases has led to a vast amount of experimental and theoretical studies.[1–3] The dominating structural pattern of amorphous and liquid Se close to the melting point is believed to consist of macromolecular chains with a length of 10^4-10^5 atoms.[4] Under these conditions, the geometry can be described by a self-avoiding random-walk model.[5] Street, Mott, and Davis (SMD) (Refs. 6 and 7) and Kastner, Adler, and Fritzsche (KAF) (Ref. 8) have extended this picture by considering possible defects within a model of local chemical bonding and an effective electron-electron attraction.[9] In the SMD model, bonds can be broken heterolytically and give rise to charged, singly coordinated D^+ (or $C_1{}^+$) and D^- (or $C_1{}^-$) defects. Following KAF, the former is supposed to form a chemical bond with an atom exhibiting a twofold coordination, and thus gives rise to a defect with three neighbors, a $C_3{}^+$ center. Experimental evidence for this picture stems from photoinduced electron spin resonance (ESR) spectroscopy,[10,11] optical absorption measurements,[8,12–14] ^{77}Se NMR spectroscopy,[15] thermodynamic data,[16] x-ray scattering,[17,18] neutron diffraction,[19] and from the chemical synthesis and structural analysis of polyions which contain chalcogen atoms with a coordination number different from 2.[20–23] Computer simulations also suggest the existence of a considerable fraction of C_1 and C_3 defects for the liquid and amorphous phase of Se.[24–42]

In this work, we aim to attain a physically transparent model of the topology and the electronic structure of disordered Se which preserves its main physical and chemical features. To describe aggregates of Se with coordination numbers larger than 2 implies the introduction of branching elements into a chainlike random-walk picture. From our perspective, models based upon small world network (SWN) ideas[43] are prospective candidates for generating such cross-linked topological structures in a simple manner. We extend the SWN concept to model liquid and amorphous Se, which allows us a broad variation of the defect concentration underlying the electronic structure.

One has to account for the topological connectivity of the network, i.e., to reflect for each realization unambiguously whether each pair of atoms is chemically bonded or not. Furthermore, within a tight-binding description of the chemical bond each atom has to display the correct orbital hybridization corresponding to the chemical bonds to which it belongs. The first aspect is of common occurrence in many physical models; one is led to a connectivity matrix. A special case of this approach is provided in polymer science by extensions of the classical Rouse model to generalized Gaussian structures (GGS's).[44,45] On the other hand, the proper consideration of the chemical situation of each Se atom is an additional feature which we take into account here. In contrast to models based on Cayley trees or Bethe lattices, surface effects do not play a dominant role in the networks presented here, and the influence of closed loops of different sizes on the electronic structure can be studied. The electronic structure is described by a tight-binding Hamiltonian, which is extended by an effective electron-electron interaction. With a basis of three $4p$ orbitals per site, it is chemically correct and closely follows the original concepts put forward by SMD and KAF. For one-dimensional disordered chain models of Se, this Hamiltonian has found a recent application.[46]

Our paper is organized as follows: In the next section we describe the procedure to generate small world networks specific to the bond topology encountered for Se and the tight-binding model underlying the electronic structure computations. Numerical results including the density of states, the location and origin of defects within the density of states, charge distributions, and localization properties are described in Sec. III. The results are discussed, and conclusions are derived in the final section.

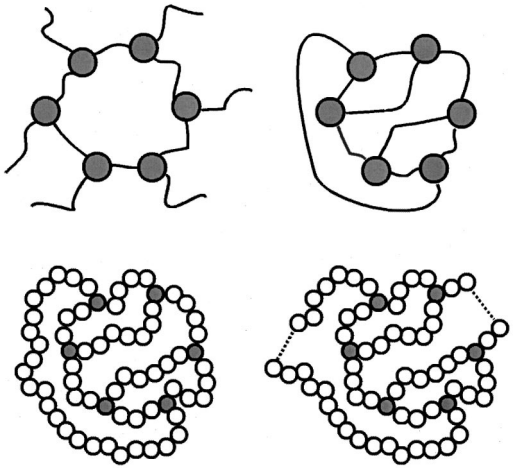

FIG. 1. Construction scheme for a modified small world network containing six C_3 centers, four C_1 centers, and 56 atoms with a twofold coordination. From top left to bottom right: regular chain of prospective C_3 centers with cyclic boundary conditions and dangling bonds; random linkage of the dangling bonds; insertion of C_2 atoms; introduction of pairs of C_1 defects.

II. METHODS

In the following, we specify the topological structures which we aim to address. Given that in the absence of defects the Se atoms form chains, it is tempting to assume that the defects are realized as additional chemical bonds between the atoms. This idea leads directly to the concept of so-called small world networks, which are of considerable recent interest.[43] Namely, the concept of a regular lattice having equiprobable additional bonds between arbitrary pairs of sites—thus defining the SWN concept—has provided a different outlook on general network structures, ranging from internet links[47] to the spread of infections.[48] Basic physical phenomena such as classical transport are associated with problem of determining the eigenvalues and eigenvectors of the corresponding Laplacian; these problems have also been studied for SWN's.[49,50] In this way, SWN's have turned out to be a particularly useful concept in polymer chemistry and physics, where they provide interesting insight into polymer relaxation and diffusion.[51,52]

In this work we consider networks consisting of n atoms with a standard coordination number of 2. In addition, there exist defects with a threefold coordination (C_3 centers) which act as cross links, and C_1 centers which terminate branches of the random network. To generate networks with a nonvanishing number n_3 of C_3 centers, we start from a ring of n_3 Se atoms with twofold coordination and a dangling bond each; see Fig. 1. Of these n_3 bonds, $n_3/2$ pairs are drawn at random and interconnected, a step very akin to the formation of SWN's, where—apart from the nearest-neighbor bonds—each center is connected with probability unity to another center. The so created C_3 backbone of the network is completed by randomly inserting additional $n-n_3$ Se atoms into existing Se-Se bonds. A schematic representation of this process is presented in Fig. 1. Within the network, the formation of two consecutive σ bonds has to be avoided. This configuration would imply a bond angle of 180°, an unphysical requirement considering the experimental finding of 103.1° and the 90° value underlying our local $\{p_x, p_y, p_z\}$ orbital basis and its decoupling. Hence a minimum number of two atoms with a twofold coordination has to be inserted into each pair of C_3 centers. As a last step, an even number n_1 of C_1 centers is generated by breaking $n_1/2$ bonds between Se atoms which are characterized by the coordination number $Z=2$. The largest possible number of C_3 defects introduced into the SWN equals $n/4$; for this configuration, the maximum fraction of C_1 defects equals $3n/4$. Computer simulations of liquid Se applying a three-body potential based on *ab initio* calculations suggest fractions of defects smaller than 0.27 for the C_1 defects and 0.07 for the C_3 defects close to the critical point.[27] Defect concentrations in tight-binding molecular-dynamics studies exhibit maximum values of 0.2 for both C_1 and C_3 defect concentrations.[32] Consequently, the number density of defects obtainable within our model can be considered as sufficient for all practical purposes. The insertion of C_2 centers and the creation of C_1 defects model chemical requirements for Se networks and lead to a departure from the classical SWN scheme. For very large networks one may have to check whether the model stays within the SWN class. Given, however, that the number of centers we use is not extremely large, we dispense here with an in-depth analysis.

To describe the electronic structure, we start from a simple tight-binding Hamiltonian. In second quantization, it reads

$$\hat{H}=\sum_{a\neq b}\sum_{i,j} a_{ia}^{+}a_{jb}V_{iajb} \tag{1}$$

with a basis of three $4p$ orbitals localized on each Se atom and where the V_{iajb} vanish if the atoms a and b are not chemically connected. As in most simplified treatments of Se, the low-lying $4s$ orbitals are ignored. The a_{ia}^{+}/a_{jb} denote creation/annihilation operators acting upon atomic orbitals i,j localized on atoms a,b. From the parametrization of Bichara *et al.*,[34] we obtain hopping matrix integrals of $V_{pp\sigma}=2.95$ eV for σ and $V_{pp\pi}=-0.78$ eV for π bonds. We assume a bond angle of $\pi/2$ and dihedral angles of zero, $\pi/2$, π, and $3\pi/2$. From the point of view of the electronic structure, the model exhibits a local Cartesian geometry. Consequently, the three p orbital problems can be separated if only nearest-neighbor interactions are taken into account. In the case of bond angles different from 90°, the p orbital problems do not separate any more, and hopping matrix elements have to be weighted by the direction cosines according to the Slater–Koster rules.[53]

Electron correlation is introduced via the familiar Hubbard model of intraorbital electron-electron interaction.[54] The Hamiltonian (1) is extended by the term

$$\hat{H}_{\mathrm{int}}=-U\sum_{ia} n_{ia}^{2}. \tag{2}$$

In previous work based on chainlike topologies,[46] we have obtained a good agreement with the experimental band gap for a spin pairing energy $U_{\mathrm{SP}}=2$ eV. For closed-shell systems—as encountered here—this spin pairing energy is

equivalent to an attractive Hubbard parameter of $U = 0.5$ eV once the complete electronic charge order within an orbital is considered via the spin-free number operators n_{ia}. The resulting many-body problem is solved self-consistently at the Hartree-Fock mean-field level,

$$n_{ia}^2 \approx 2n_{ia}\langle n_{ia}\rangle - \langle n_{ia}\rangle^2, \tag{3}$$

following the procedure given in Ref. 55. In Eq. (3), the brackets indicate averaging with respect to the ground state, in this case calculated from a previous step of the SCF procedure. The U value applied here is identical to the estimate of Feltz,[56] and slightly smaller than that given by Larmagnac *et al.* (0.95 eV, Ref. 57) and values obtained for chalcogenide glasses (0.7–0.8 eV, Ref. 58).

In the presence of defects, we are interested in the partial density of states with reference to the defect species C_X ($X = 1,3$); this quantity can be computed by averaging within an energy interval over the appropriate charge orders,

$$q_\alpha = \sum_{ia}{}' \; c_{ia\alpha}^2. \tag{4}$$

In Eq. (4), the $c_{ia\alpha}$ denote the expansion of an eigenstate $|\alpha\rangle$ in terms of the basis functions $|ia\rangle$. The partial density of states (PDOS) is defined as the product of the charge order and the density of states (DOS). As a suitable localization measure—which is independent of the geometry of the system—we make use of the inverse participation ratio,[59]

$$P_\alpha = \sum_{ia} \; c_{ia\alpha}^4. \tag{5}$$

The inverse participation ratio equals unity for states confined to a single atomic orbital and can be interpreted as the inverse of the number of basis functions over which an eigenstate is spread.

It befits now to point out the aspects which we neglect in our model. Clearly neglected is the slow dynamics of the network, a problem which requires for its study long molecular-dynamic runs or sophisticated Monte Carlo techniques;[60,61] we argue—as usual in condensed-mater physics—that the electronic and phononic degrees of freedom can be separated. Focusing only on the local chemical situation and on the long-range network topology allows us, as we proceed to show, to obtain a very transparent model with clearly defined coordination numbers (and hence defect types) at every site and thus to monitor in a straightforward manner the defect concentration. In doing so we can take—even for quite large systems—a considerable number of particular realizations into account and hence can well assess the role of the disorder.

III. RESULTS AND DISCUSSION

We have obtained numerical results obtained for models containing 64, 120, and 360 atoms each; a list of the models discussed in this paper is given in Table I. For a given number of atoms and defects, we have investigated 50–1000 different realizations, depending on the rate of convergence of the self-consistent field iteration procedure. Although our model does not explicitly include the influence of the temperature (i.e., whether the state of Se is amorphous or fluid) such an aspect is implicitly included through the defect concentrations which are used. None of the properties show a pronounced dependence of the system size within the range of 64–360 atoms. In this work, mainly data based on systems containing 120 atoms have been used for the following reasons. First, and most important, they allow the computations of properties based on a larger number of systems as those containing 360 atoms. This holds in particular for the partial charge distributions displayed below. Second, all defects have finally turned out to be localized; as a consequence, rather small systems provide a sufficient description. The densities of states are not affected by increasing the system size. The defect concentrations used here have been deliberately set to large values in order to obtain proper statistics for the properties of the associated defect species.

TABLE I. List of models presented in Figs. 2–4.

Atoms	C_1 defects	C_3 defects	Boundary conditions	U [eV]	Figure/ model	Realizations
64			cyclic	zero	2(a)	1000
120			cyclic	0.5	2(b)	100
64	2		open	0.5	2(c)	100
120		20	cyclic	zero	3(a)	100
360		60	cyclic	0.5	3(b)	50
120		20	cyclic	0.5	3(b), 4(a)	100
120	10	20	cyclic	0.5	3(c), 4(b)	100

With the help of Fig. 2, we illustrate the densities of states typical for systems based upon the topology of *linear* chains. In the absence of electron-electron interactions and in the presence of cyclic boundary conditions, the density of states of the Se models studied here exhibits the familiar structure of an occupied σ band, an occupied π band, and a vacant σ^* band, all separated by band gaps [Fig. 2(a)]. The Fermi level is located in the gap between the π and the σ^* band. In comparison with the experimental value of the gap, $E_{\mathrm{gap}} = 2$ eV,[62] the theoretical value of 0.4 eV is rather small. In the absence of cyclic boundary conditions, two C_1 centers terminate the Se chain. Due to the lack of one σ bond, the Fermi level is shifted into the valence band, leaving two vacant states. The implications of this Fermi level shift for an ensemble of disordered chains have been discussed in detail by Koslowski and von Niessen.[64] In the presence of an attractive interaction of the Hubbard type ($U = 0.5$ eV), all occupied bands are shifted into the red, as illustrated in Fig. 2(b) for a chain with cyclic boundary conditions. The π band, having the lowest kinetic energy, experiences a stronger influence of the electron-electron interaction, its shift is more pronounced than that of its σ counterpart. This fact leads first to an increase of the gap between the π and the σ^* band to 1.8 eV, and second to the merging of the σ and the π band. Once C_1 defects are introduced by breaking a bond, the behavior observed by one of the present authors for various random-walk models of the disordered phases of Se is recovered:[46] a narrow and pronounced impurity band is formed close to the zero of energy, E_F now lies between the

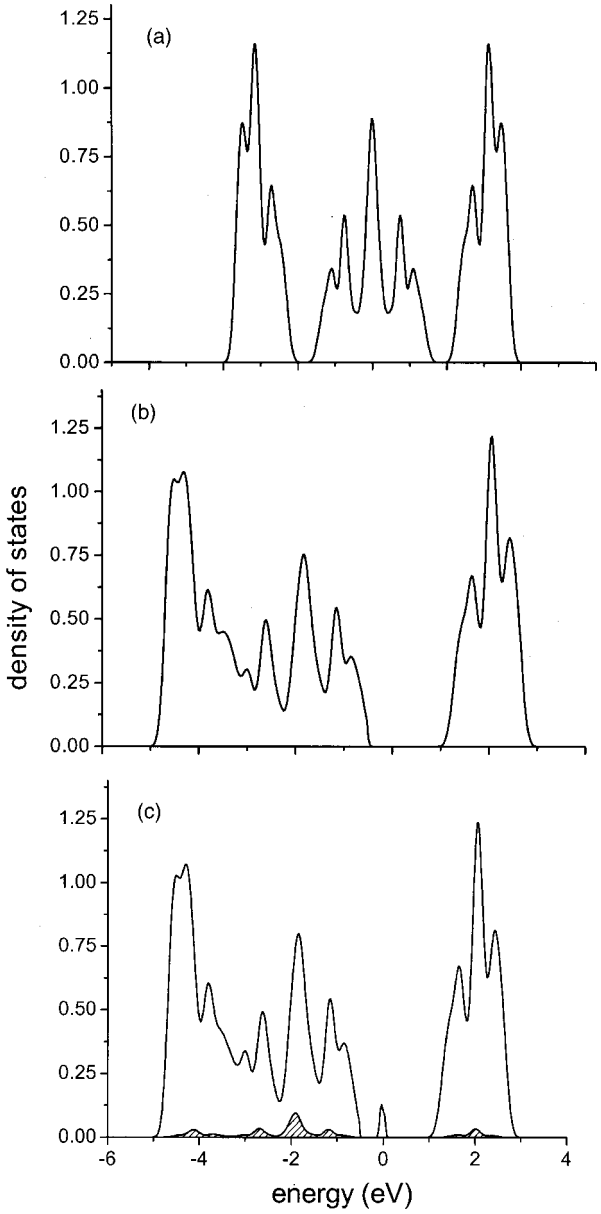

FIG. 2. Density of states for random walk models. (a) cyclic boundary conditions, $U=0$; (b) cyclic boundary conditions, $U=0.5$ eV; (c) Dirichlet boundary conditions, $U=0.5$ eV. The defect density of states has been shaded. Energy in electron volts, density of states per atom and electron volt.

π band and the impurity band [Fig. 2(c)]. A thorough analysis of the underlying partial density of states and the charge distribution within the chain has revealed that the C_1 centers are negatively charged, in contrast to the conjecture of Street and Mott.[6,7] The negative charge is compensated by the formation of a bipolaron exhibiting a twofold positive charge. The atomic orbitals that are characterized by the smallest electron population experience the weakest electron-electron interaction and are thus shifted to the blue with reference to the π valence band. The impurity band has to be interpreted as a bipolaron band,[46] whereas the chain end atomic orbitals only contribute to a broad defect partial density of states within the bulk DOS, concomitant with a vanishing defect PDOS within the bipolaron band.

The densities of states for the simple chain models in Figs. 2(a) and 2(c) are based on similar sets of eigenstates as in Ref. 46. In that work, the spectra have been accumulated in coarse-grained histograms, whereas the densities of the states in the present paper are obtained by a Gaussian broadening of the energy levels.[63] This gives rise to a better resolution of the fine structure of the DOS. Figure 2(a) of the present paper is computed using the same program as applied in Ref. 46, and so closely resembles Fig. 2(a) presented there. Figure 2(c) of this paper finds its counterpart in Fig. 3(b) of Ref. 46, only the number of neighbors (two nearest vs four nearest and next nearest) differ. In any case, the main physical features, i.e., bandwidths and gaps, are identical. The densities of states presented in Figs. 2(b) and 3(a)–(c) do not find counterparts in Ref. 46.

We now turn to the results of our SWN-type model, which describes systems containing C_3 defects, whose influence upon the densities of states is illustrated in Fig. 3. In the absence of interactions, the density of states close to the Fermi level is not altered significantly [Fig. 3(a)], the σ and π bands can be clearly distinguished. There is no sign of the formation of isolated defect bands within the band gap of the unperturbed system. Nevertheless, we find satellite peaks both in the high- and in the low-energy part of the spectrum, which are characterized by a large C_3 partial density of states. Throughout this work, we have assumed perfect local order, i.e., ideal bond angles of 90° and dihedral angles of zero, 90°, 180°, or 270°. In a more realistic model, these values have to be replaced by the corresponding distributions. Deviations from the mean values will effect the electronic matrix elements via the direction cosines via the Slater-Koster rules.[53] The resulting density of states is also presented in Fig. 3(a). It is characterized by a Gaussian bond angle distribution with an rms value of 15°, which corresponds to the largest value observed in the Monte Carlo simulations described above.[27] Within our model, deviations from an ideal bond angle basically lead to a small nonzero density of states within former band gaps and to the enhancement of nonbonding contributions, most pronounced in the π^0 band.

If defects with a threefold coordination are introduced to a model which takes electron-electron interactions into account, an impurity band is formed within the former band gap, and the Fermi level of the effective one-electron problem can again be located between the π valence band and the impurity band [Fig. 3(b)]. The impurity band is split into a larger lower and a smaller upper band, with defect partial densities of states that are approximately equal. Upon the additional introduction of C_1 defects, the density of states of the lower part of the impurity increases, until at a sufficiently high fraction of dangling bonds these bands finally merge [Fig. 3(c)]. With the help of Fig. 3(b), we also demonstrate that system size effects on the density of states play a minor role.

To get additional insight into the nature of defect states, we have analyzed the charge distributions of systems characterized by a nonvanishing value of U. This analysis is depicted in Fig. 4. We present partial charge distribution functions, which display the contribution of specific types of defects to the total charge distribution. For systems free of

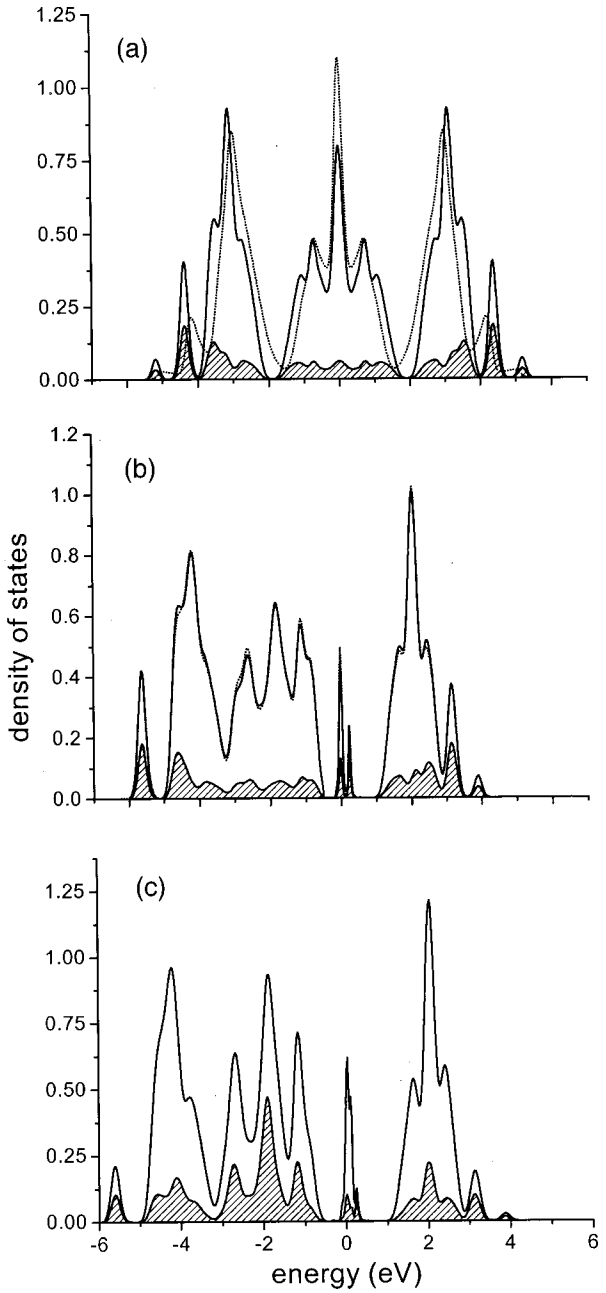

FIG. 3. Density of states and defect partial density of states (shaded) for small world networks. (a) C_3 centers, $U=0$ (dotted: off-diagonal disorder); (b) C_3 centers, $U=0.5$ eV (DOS: full line, 120 atoms, dotted: 360 atoms); (c) C_1 and C_3 centers, $U=0.5$ eV. Energy in electron volts, density of states per atom and electron volt.

defects, fluctuations around the average value of zero are small. Once two C_1 centers are present, the formation of negatively charged chain ends can be observed as a peak at $q=-1$, and the asymmetric charge distribution within the bipolaron is manifest in two peaks. For systems consisting of cross-linked chains, the charge distributions are considerably broadened. Their main features, however, can still be understood in a direct manner. In the absence of C_1 defects, the C_3 partial charge distribution functions exhibits two broad maxima in the range of positive charges. The defects exhibiting positive charges around unity correspond to the C_3^+ center postulated by Kastner, Adler, and Fritzsche.[8] The broad maximum in the defect partial charge distribution function in the interval $0<q<0.75$ corresponds to C_3 centers with a smaller positive charge: a more elaborate population analysis reveals that these states belong to the lower of the two impurity bands. The C_2 charge distribution can also be characterized as bimodal, the C_3 positive charges are compensated by a second maximum at $q=-0.5$ [Fig. 4(a)]. Systems containing both C_1 and C_3 defects exhibit the characteristic signatures of both defect types in the charge distribution, i.e., the influence of the C_1 and C_3 center charges is not simply compensated so as to cancel each other.

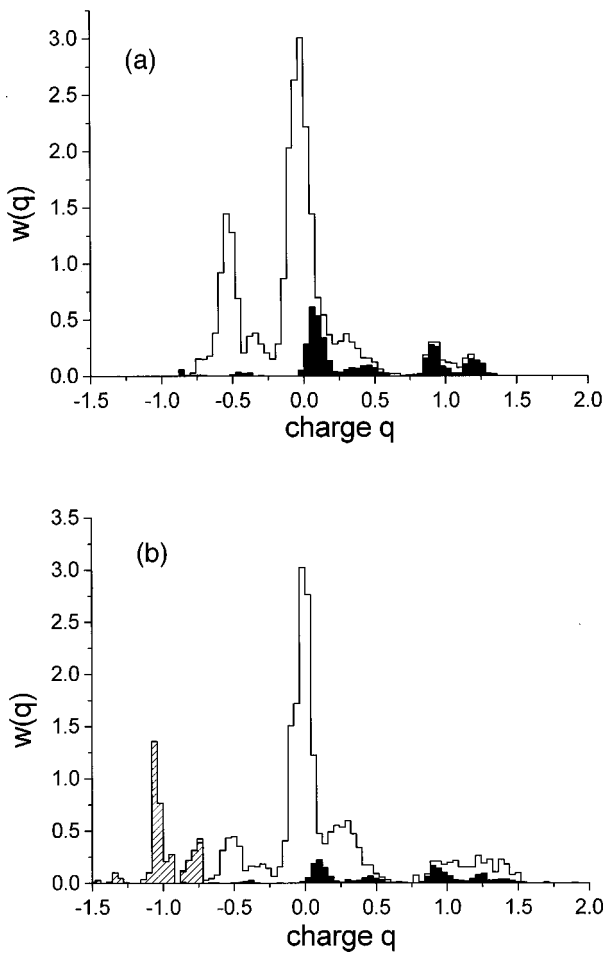

FIG. 4. Total and partial charge distribution functions for interacting models with $U=0.5$ eV. (a) C_3 defects only; (b) C_3 and C_1 defects. C_3 partial charge distribution, black; C_1 partial charge distribution, shaded.

The localization measures of the models presented here are listed in Table II. Whenever impurity bands are present, their inverse participation ratio is notably larger than that of the bulk σ and π bands. This holds in particular for the C_3^+ upper impurity band: it exhibits both localized eigenstates and localized charges. Bipolaronic defects and C_3 centers with a small positive charge are more extended, and the localized C_1^- charges give rise to a small contribution to averages of localization measures within the bulk density of states.

TABLE II. Inverse participation ratio, averages taken with reference to the following energy bands (in eV). Interacting systems: σ $[-5,-3]$, π $[-3,-0.5]$, lower impurity $[-0.5,0.1]$, upper impurity [0.1,0.5], and σ^* [0.5,3]. Noninteracting systems: σ $[-4,-2]$, π $[-2,2]$, and σ^* [2,4].

Model	σ	π	Lower impurity	Upper impurity	σ^*
2(a)	0.16	0.21			0.20
2(b)	0.13	0.19			0.17
2(c)	0.14	0.21	0.27		0.18
3(a)	0.16	0.17			0.16
3(b)	0.14	0.15	0.20	0.32	0.17
3(c)	0.19	0.26	0.25	0.41	0.24

As we mainly use models characterized by ideal local order, the densities of states obtained here have to be compared with more elaborate computations on systems exhibiting the same feature. We take the gradient-corrected density-functional *ab initio* computations of Kirchhoff *et al.*[42] on trigonal Se as a reference, which is also well reproduced by the tight-binding model of Molina and co-workers.[33] The band gap of 1.8 eV computed here is larger than that of the density functional theory (DFT) calculations (1.3 eV), yet closer to the experimental value of 2 eV. This may reflect the well-known fact that DFT tends to underestimate the band gap for semiconductors by approximately 40%,[65] whereas the opposite tendency holds for *ab initio* Hartree-Fock calculations. The bandwidths within the singly coordinated densities of states [Fig. 2(b)] are smaller than those of the *ab initio* computations; we note a σ^* conduction bandwidth of 1.9 eV, as compared to 2.8 eV, and a total width of the valence band of 4.1 eV, compared to 5.7 eV. In either case, the bands exhibit a pronounced fine structure. Once the effective number of neighbors is increased—as encountered here in computations of models containing C_3 centers, cf. Fig. 3(b)—the bulk bands are broadened by satellites to values closer to that of the reference computations and tight-binding calculations with hopping matrix elements extending beyond nearest neighbors. We now obtain a valence-band width of 5.3 eV and a conduction-band width of 2.8 eV.

The formation of valence alternation pairs and the associated formation of single positive or negative charges have also been attested in recent tight-binding molecular-dynamics studies of liquid Se,[37] but no attempt has been made in the work just referenced to correlate them to specific coordination numbers or to identify their location within the densities of states. We note that Lomba *et al.* have also introduced a Hubbard correction to remove minor deficiencies from their tight-binding model.[37] This interaction, however, is of a repulsive character and penalizes charge alternations. It is treated within first-order perturbation theory to compute the Hellmann-Feynman forces within the molecular-dynamics simulation. As a consequence, the number of valence alternation pairs as manifest in the total charge distribution curves decreases compared to the simple interaction-free tight-binding model.

IV. CONCLUSIONS

In this work, we have presented a modified small world network approach to the geometry and electronic structure of Se in its disordered phases. Within this model, C_3 and C_1 defect centers as postulated in the literature and encountered in molecular-dynamics simulations can be introduced in a controllable way within a broad range of concentrations. The small world network concept has been extended to take the nature of the chemical bond in the disordered phases of Se into account, chemical specificity has been achieved by an algorithm that excludes configurations with two consecutive σ bonds and by providing a basis set of three $4p$ orbitals. The electronic structure has been described by a nearest-neighbor tight-binding Hamiltonian, which has been extended by a Hubbard term to take an effective electron-electron interaction into account. With the help of the restricted Hartree-Fock approximation, self-consistent solutions have been obtained for polyselenium chains and networks.

Once the effective electron-electron interaction becomes operative, the narrow band gap between the π valence and the σ^* conduction band is widened to a value of around 1.8 eV, which is comparable to experimental data.[62] Defect states within the gap are only observed for a nonvanishing Hubbard U parameter for systems containing C_1 and C_3 defects. In the presence of C_1 defects only, states within the gap do not exhibit a significant defect partial density of states, and the impurity band can be attributed to bipolaronic charges within the Se chains.[46] The C_3 defects give rise to an additional impurity band, coinciding in energy with the bipolaron band. In contrast to the bipolaron impurity band, its C_3 counterpart is characterized by a large partial defect density of states. In terms of the inverse participation ratio and compared to the bulk density of states, all defect states show a higher degree of localization.

To summarize, we have investigated the total and partial charge distributions arising from the introduction of defects, concluding that within the former band gap three different types of impurity bands exist: bipolaronic, C_3^+, and also C_3 with a small positive charge (which we may refer to as $C_3^{\delta+}$). Moreover, there also exist C_1^- defects, but they are not manifest as an impurity band. The energetic sequence of the impurity bands can be rationalized in terms of their charge, those with large positive charge experience the effective electron-electron attraction to a smaller degree than negatively charged defects do. Thus positively charged impurity bands lie at higher energies than their negatively charged counterparts.

ACKNOWLEDGMENTS

It is a pleasure to thank D. Marx (Bochum), M. Epple (Bochum), V. Staemmler (Bochum), K. Fink (Bochum), W. Freyland (Karlsruhe), and T. Cramer (Freiburg) for stimulating and fruitful discussions. We gratefully acknowledge support by the Deutsche Forschungsgemeinschaft. A Blumen thanks the Fonds der Chemischen Industrie for its support.

*Corresponding author. Fax: (+49)-761-203-6189; email address: Thorsten.Koslowski@physchem.uni-freiburg.de

[1] *Selenium*, edited by R. A. Zhigaro and W. C. Cooper (Van Nostrand, New York, 1974).
[2] *Selenium and Tellurium*, edited by E. Gerlach and P. Grosse (Springer-Verlag, Berlin, 1979).
[3] F. Hensel and W. W. Warren, *Fluid Metals* (Princeton University Press, Princeton, NJ, 1999).
[4] R. C. Keezer and M. W. Bailey, Mater. Res. Bull. **2**, 158 (1967).
[5] R. Bellisant and G. Tourand, in *Proceedings of the 7th Conference on Liquid and Amorpous Semiconductors*, edited by W. E. Spear (University of Edinburgh, Edinburgh, 1977), p. 98; after R. Bellisant and G. Tourand, J. Non-Cryst. Solids **35–36**, 1221 (1980); M. Misawa and K. Suzuki, J. Phys. Soc. Jpn. **44**, 162 (1978).
[6] R. A. Street and N. F. Mott, Phys. Rev. Lett. **35**, 1293 (1975).
[7] N. F. Mott, E. A. Davis, and R. A. Street, Philos. Mag. **32**, 961 (1975).
[8] M. Kastner, D. Adler, and H. Fritzsche, Phys. Rev. Lett. **37**, 1504 (1976).
[9] P. W. Anderson, Phys. Rev. Lett. **34**, 953 (1975).
[10] S. G. Bishop and U. Strom, Conf. High. Transp. Mat., Atlanta, 1976, after Feltz (Ref. 56).
[11] F. Mollot, J. Cernegora, and C. Benoit, Philos. Mag. B **42**, 643 (1980).
[12] S. G. Bishop, U. Strom, and P. C. Taylor, Phys. Rev. **15**, 2279 (1977).
[13] S. G. Bishop, U. Strom, and P. C. Taylor, Philos. Mag. B **37**, 241 (1978).
[14] P. C. Taylor, S. G. Bishop, and U. Strom, Phys. Rev. **18**, 511 (1978).
[15] W. W. Warren and R. Dupree, Phys. Rev. B **22**, 2257 (1980).
[16] G. Weser, W. W. Warren, and F. Hensel, Ber. Bunsenges. Phys. Chem. **82**, 588 (1978).
[17] M. Misawa and K. Suzuki, Trans. Jpn. Inst. Met. **18**, 427 (1977).
[18] Y. Soldo, J. L. Hazemann, D. Aberdam, M. Inui, K. Tamura, D. Raoux, E. Pernot, J. F. Jal, and J. Dupuy-Philon, Phys. Rev. B **57**, 258 (1998).
[19] M. Edeling and W. Freyland, Ber. Bunsenges. Phys. Chem. **85**, 1049 (1981).
[20] R. J. Gillespie, R. Burns, and J. Sawyer, Inorg. Chem. **19**, 1423 (1980).
[21] D. Fenske, G. Kräuter, and K. Dehnicke, Angew. Chem. **102**, 421 (1990).
[22] B. E. Krebs, E. Lührs, R. Willmer, and F.-P. Ahlers, Z. Anorg. Allg. Chem. **17**, 529 (1991).
[23] W. S. Sheldrick and H. G. Braunbeck, Z. Naturforsch. B **44**, 1397 (1987).
[24] N. G. Almarza, E. Enciso, and F. J. Bermejo, J. Chem. Phys. **99**, 6876 (1993).
[25] S. Balasubramanian, K. V. Damodaran, and K. J. Rao, Chem. Phys. **166**, 131 (1992).
[26] C. Oligschleger, R. O. Jones, S. M. Reimann, and H. R. Schober, Phys. Rev. B **53**, 6165 (1996).
[27] Th. Koslowski, Z. Phys. Chem. (Munich) **210**, 45 (1999).
[28] R. Bruning, E. Irving, and G. Leblanc, J. Appl. Phys. **89**, 3215 (2001).
[29] D. Caprion and H. R. Schober, J. Chem. Phys. **114**, 3236 (2001).
[30] D. Caprion, J. Matusi, and H. R. Schober, Phys. Rev. Lett. **85**, 4293 (2000).
[31] D. Caprion and H. R. Schober, Phys. Rev. B **62**, 3709 (2000).
[32] E. Lomba, D. Molina, and M. Alvarez, Phys. Rev. B **61**, 9314 (2000).
[33] D. Molina, E. Lomba, and G. Kahl, Phys. Rev. B **60**, 6372 (1999).
[34] C. Bichara, A. Pellegatti, and J.-P. Gaspard, Phys. Rev. B **49**, 6581 (1994).
[35] J. Y. Raty, A. Saul, J. P. Gaspard, and C. Bichara, Comput. Mater. Sci. **17**, 239 (2000).
[36] R. Stadler, D. R. Bowler, D. Alfe, and M. J. Gillan, J. Phys.: Condens. Matter **12**, 5109 (2000).
[37] E. Lomba, D. Molina, and M. Alvarez, Phys. Rev. B **61**, 9314 (2000).
[38] D. Hohl and R. Jones, Phys. Rev. B **43**, 3856 (1991); J. Non-Cryst. Solids **117–118**, 922 (1990).
[39] F. Kirchhoff, M. J. Gillan, J. M. Holender, G. Kresse, and J. Hafner, J. Phys.: Condens. Matter **8**, 9365 (1996).
[40] F. Shimojo, K. Hoshino, M. Watabe, and Y. Zempo, J. Phys.: Condens. Matter **10**, 1199 (1998).
[41] H. Ohtani, T. Yamagutchi, and F. Yonezawa, J. Phys. Soc. Jpn. **69**, 3885 (2000).
[42] F. Kirchhoff, G. Kresse, and M. J. Gillan, Phys. Rev. B **57**, 10 482 (1998).
[43] D. J. Watts and S. H. Strogatz, Nature (London) **393**, 440 (1998).
[44] J.-U. Sommer and A. Blumen, J. Phys. A **28**, 6669 (1995).
[45] P. Biswas, R. Kant, and A. Blumen, Macromol. Theory Simul. **9**, 56 (2000).
[46] Th. Koslowski, J. Phys.: Condens. Matter **9**, 613 (1997).
[47] R. Albert, H. Jeong, and A. L. Barabasi, Nature (London) **401**, 130 (1999).
[48] C. F. Moukarzel, Phys. Rev. E **60**, R6263 (1999).
[49] R. Monasson, Eur. Phys. J. B **12**, 555 (1999).
[50] S. Jespersen, I. M. Sokolov, and A. Blumen, J. Chem. Phys. **113**, 7652 (2000).
[51] S. Jespersen, I. M. Sokolov, and A. Blumen, Phys. Rev. E **62**, 4405 (2000).
[52] S. Jespersen and A. Blumen, Phys. Rev. E **62**, 6270 (2000).
[53] J. C. Slater and G. F. Koster, Phys. Rev. **94**, 1498 (1954).
[54] J. Hubbard, Proc. R. Soc. London, Ser. A **276**, 238 (1963); **281**, 401 (1964).
[55] Th. Koslowski, J. Chem. Phys. **113**, 10703 (2000).
[56] A. Feltz, *Amorphous Inorganic Materials and Glasses* (VCH, Weinheim, 1993), p. 133.
[57] J. Larmagnac, P. Carles, and G. Lefrancois, J. Non-Cryst. Solids **77–78**, 1237 (1985).
[58] W. Kastner and H. Fritzsche, Philos. Mag. **37**, 199 (1978).
[59] D. J. Thouless, Phys. Rep. **13**, 93 (1974).
[60] F. T. Wall and F. Mandel, J. Chem. Phys. **63**, 4592 (1975).
[61] P. G. de Gennes, J. Chem. Phys. **55**, 572 (1971).
[62] S. R. Elliott, *The Physics of Amorphous Materials*, 2nd edition (Longman, Harlow, Essex, England, 1990), p. 380.
[63] The densities of states have been obtained by broadening with a Gaussian function with a rms value of 0.1 eV (bulk DOS) or 0.025 eV (impurity bands).
[64] Th. Koslowski and W. von Niessen, Phys. Rev. B **49**, 11 704 (1994).
[65] P. Fulde, *Electron Correlations in Molecules and Solids* (Springer, Berlin, 1991), p. 51.